causes of mortality, the clinical characteristics at the time of death, and the risk factors related to mortality. The results may help provide information that prevents mortality for the families of children with this disorder and for health care professionals.

Methods

In July 2009, a questionnaire was delivered to the epilepsy training hospitals that were authorized by the Japanese Society of Epilepsy, to hospitals/institutions that were authorized to train specialists from the Society of Pediatric Neurology, and to university hospitals (total: 246 hospitals). This survey allowed us to collect information about the total number of past and present patients with Dravet syndrome, the number of patients who died, and the number of patients with serious sequelae. A secondary questionnaire was sent by mail to the 26 hospitals that reported mortality cases to obtain information on the following items for each patient: (1) gender; (2) age at the onset of epilepsy (in months); (3) clinical type (typical or borderline groups) (Fujiwara et al., 2003; Oguni et al., 2005); (4) presence or absence of an *SCN1A* gene test and its results; (5) age at death; (6) Causes of mortality; (7) presence or absence of risk factors at death, such as fever/infection, bathing, seizures, and the child's state (sleep or awake); (8) frequency of seizures and of SE before death; (9) treatment regimen; (10) neurological condition; (11) electroencephalographic and neuroimaging findings; and (12) autopsy findings.

The time from the onset of epilepsy to death and the age at death were very close because of the early onset of the epilepsy; therefore, we compared the age at death between the typical and borderline groups and among the causes of death.

Prior to this study, the protocol was approved by the Tokyo Women's Medical University Ethics Review Board and by the Dravet Syndrome Prognosis Survey/Study Group Ethics Review Board.

Statistical analyses

Statistical analyses were performed using SPSS 15.0J (SPSS Japan, Tokyo, Japan) for Windows. The chi-square test, *t*-test, and Mann-Whitney *U*-test were employed to compare the results between two variables. A comparison among more than three variables was performed using the chi-square test with cross tabulation. The Bonferroni correction was added to the statistics when multiple statistical comparisons were performed between several groups. A p-value of <0.05 was regarded as significant.

Results

Subjects

Responses were collected from 147 of the 246 hospitals (response rate: 59.8%). In 91 of the 147 hospitals, a total of 623 patients with Dravet syndrome were treated (median: two patients/hospital; range 1–109/hospital). In addition, data on 63 patients who died were collected from 26 hospitals (438 patients). Of these patients, the data from 59, excluding 4 for whom the information at the time of death was insufficient, were analyzed.

Clinical characteristics of the patients who died

In the 59 patients included in the analyses, the male-to-female ratio was 26:33. The ages of the patients at the onset of epilepsy ranged from 2–10 months, with a mean of 5.1 months. Of the 59 patients included in the analyses, 20 patients comprised the borderline group without myoclonic or atypical absence seizures, and 39 patients comprised the typical group (Table 1). No significant differences were observed between the two groups for the age at the onset of epilepsy, the age at death, the causes of mortality, the frequency of seizures before death, or the number of antiepileptic drugs ($p > 0.05$). In the typical group, the frequency of seizures before death was slightly higher than that in the borderline group, and the rates of mental retardation were slightly higher; however, there were no significant differences in the rates of severe mental retardation between the two groups ($p > 0.05$). The number of antiepileptic drugs, the frequency of seizures, and the grade of mental retardation were unclear or not described for three patients, three patients, and one patient, respectively.

Mortality

For the 26 hospitals that reported at least one patient who died for this nationwide survey, mortality accounted for 14.4% of their patients with Dravet syndrome (63 of 438 patients). When using the 91 hospitals (623 patients) as a denominator population, the prevalence of death was 10.1%.

Causes of mortality and age distribution

The patients' ages at the time of death ranged from 13 months to 24 years and 11 months, with a median age of 6 years and 8 months. The ages were distributed most frequently between 13 months and approximately 12 years and were rarely older in both the typical and borderline groups (Fig. 1). The distribution of the time between the two groups did not differ significantly ($p = 2.88 > 0.05$).

The causes of mortality were largely classified into three groups: sudden death (n = 31, 53%), acute encephalopathy with SE (n = 21, 36%), and drowning (n = 6, 10%). The remaining one patient died of fulminant hepatitis B (1%). When reviewing the age distribution with respect to the causes of mortality, two characteristic patterns were observed (Fig. 2). Briefly, the prevalence of sudden death reached a first peak at 1–3 years of age and a second small peak at 18 years and older. In contrast, the prevalence of acute encephalopathy with SE was prevalent between

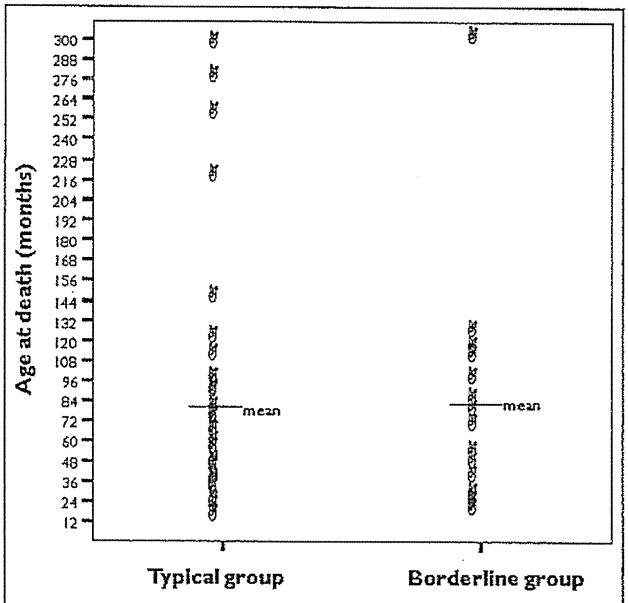

Figure 1.
Dot plots showing the distribution of age at death in the typical and borderline groups (n = 59). The age at death appeared prevalent between 13 and 140 months of age and sparse thereafter in both typical and borderline groups. No significant difference was observed between these two groups ($p > 0.05$).
Epilepsia © ILAE

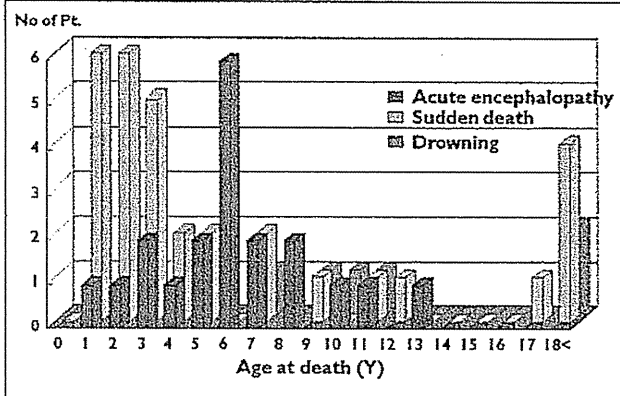

Figure 2.
Distribution of ages at death with respect to the causes of mortality. The incidence of sudden death reached a first peak at 1–3 years old and a second small peak at 18 years and older. In contrast, the acute encephalopathy-related mortality rate reached a sharp peak at 6 years old. All patients were 7 years old or older in the drowning group.
Epilepsia © ILAE

approximately 3 and 8 years of age with a sharp peak at age 6.

Causes of mortality and clinical features

The causes of mortality were associated with fever and the age at death (Table 2). In the sudden death group, the median age at death was 43 months, which was lower than that (72 months) in the acute encephalopathy group. These two groups exhibited characteristic age distributions with different peaks ($p < 0.05$), that is, the sudden death group was more likely to die at an age <47 months and after 168 months, whereas the acute encephalopathy group was more likely to experience death between 48 and 167 months (Table 2). In 81% of the patients who died of acute encephalopathy with SE, fever was noted at the time of death. In addition, fever was observed in 26% of the patients who died suddenly ($p < 0.05$). Twenty (65%) and eight (26%) of the 31 patients in the sudden death group were found to have died during sleep (or in the early morning) and during the daytime, respectively. For the remaining three patients, information about the exact time at their deaths was not available.

In 6 of the 31 patients in the sudden death group, rigid limbs and trace amounts of vomit suggested that epileptic seizures or suffocation was involved in their deaths. However, an autopsy was not performed for any of these six patients who showed the rigid limbs and trace amounts of vomit; therefore, the cause of death was not specified. In 14 patients (67%) in the acute encephalopathy group, systemic involvements, such as multiple organ failure and disseminated intravascular coagulation (DIC), became evident during or after the successful treatment of SE. Therefore, the clinical response and features of SE differed from those that the children had repeatedly experienced before. This lethal febrile SE developed suddenly at a peak age of 6 years, when the seizure or SE frequency was abated, and led to coma and multiple organ failure despite vigorous treatment. The interval of time from the onset of SE until death was 24 h or less in five patients (24%), 1 week or less in six patients (29%), more than 1 week in six patients (29%), and not known for the remaining four patients (18%).

An autopsy was performed for only 6 (10%) of the 59 patients: one who died suddenly, 4 who died of acute encephalopathy with SE, and one who died of fulminant hepatitis B. For these six patients, the causes of mortality were identified as Reye syndrome for two patients and fulminant hepatitis for one patient. However, for the remaining three patients, no cause of mortality was identified, despite the autopsy.

In the six patients who died from drowning, accidents occurred while bathing at home or in the hospital. All patients were 7 years old or older, including two patients older than 18 years of age; as a result, these patients were permitted to bathe alone.

SCN1A mutation analysis

An *SCN1A* gene test was performed for only 10 of the 59 patients. Gene mutations were detected for 7 of these 10 patients. The mutation sites were scattered in the *SCN1A* gene tests that were previously reported; as a result, no

Table 1. Clinical manifestations and phenotype

	Typical (N = 39)	Borderline (N = 20)	All cases (N = 59)	p-Value*
Gender (M/F)	17/22	9/11	26/33	3.99
Age at onset (mo.)	4.9 ± 1.7	5.5 ± 2.0	5.1 ± 1.8	2.04
Age at death (mo.)	80.7 ± 73.1	79.5 ± 70.5	80.4 ± 71.6	2.88
Cause of death Sudden/status/drowning	21/15/3	10/6/3	31/21/6	2.80
Seizure frequency Daily/weekly/monthly	13/16/8	2/7/10	15/23/18	0.567
Number of AED polytherapy (<4)/2–3	15/21	6/12	23/33	4.788
Mental retardation Severe/moderate/mild	18/14/6	4/9/7	22/23/13	0.980

M, male; F, female, mo., months; AEDs, antiepileptic drugs.
*The Bonferroni collection was added to p-values.

Table 2. Comparison between those with sudden death and acute encephalopathy

	Sudden death (N = 31)	Acute encephalopathy (N = 21)	p-Value*
Gender (M/F)	18/13	5/16	0.42
Phenotype (typical/borderline)	21/10	15/6	8.0
Age at death (mo.) ≤47 or ≤168/48–167	22/9	5/16	0.01*
Fever at death (%)	25.8	81.0	0.00*
Seizure frequency Daily/weekly/monthly	8/11/7	7/5/9	3.69
Mental retardation Severe/moderate/mild	12/10/9	7/9/4	2.16
AED polytherapy <4 (%)	32.3	38.1	4.86
Epileptic EEG abnormality (%)	56.7	42.1	4.50
Neuroimaging abnormality (%)	29.0	33.3	5.13

M, male; F, female, mo., months; AED, antiepileptic drug.
*The Bonferroni collection was added to p values.

mutation site that was characteristic of mortality was detected (Depienne et al., 2009; Lossin, 2009).

Discussion

In this nationwide survey, data were collected for 63 patients with Dravet syndrome who died, and data from 59 of these patients were used for the analyses. The result showed that the risk of mortality remained high up to the age of approximately 12 years of age, regardless of the clinical type, and sharply declined thereafter. The causes of mortality were classified into three types: sudden death, acute encephalopathy with SE, and accidents (mostly drowning). In particular, sudden death and acute encephalopathy with SE accounted for 53% and 31% of the causes of death, respectively.

The incidence of sudden death reached a first peak at 1–3 years of age and reached a second small peak at 18 years and older. Sudden unexpected death in epilepsy (SUDEP) has been reported to account for approximately 2–18% of all epilepsy-related deaths. Therefore, the incidence of SUDEP in this disorder is high (Gaitatzis & Sander, 2004; Tomson et al., 2008). During infancy, patients with Dravet syndrome experience recurrent febrile/afebrile SE despite vigorous antiepileptic drug (AED) treatments (Claes et al., 2001; Dravet et al., 2005). In the present study, neither the number of AEDs nor the frequency of the seizures was abnormally high immediately before death; however, no control group was established. The epileptic seizures associated with Dravet syndrome are presumably generated by epileptogenic pyramidal neurons because of an *SCN1A* mutation–mediated dysfunction of inhibitory interneurons (Yu et al., 2006; Ogiwara et al., 2007). The involvement of this channelopathy in epilepsy suggests that cardiac arrhythmia is a complication that is involved in the episodes of sudden death. Both arrhythmia and respiratory hypoventilation have been considered to be causes of SUDEP (Gaitatzis & Sander, 2004; Tomson et al., 2008). Most patients with Dravet syndrome who died suddenly were found in bed early in the morning or after sleeping in the afternoon. This result is consistent with common-type SUDEP. Neither electrocardiographic abnormalities nor heart/respiratory dysfunction has been reported in any children with this disorder. Unfortunately, no study has demonstrated any other arrhythmia-associated gene mutations in patients with Dravet syndrome. More work is needed to clarify whether the *SCN1A* mutation site is associated with sudden death in Dravet syndrome.

The mortality rate resulting from acute encephalopathy with SE reached a sharp peak at 6 years old (prevalent between 4 and 8 years of age). In these cases, coma or multiple organ failure led to a fatal outcome despite seizure control. Recently, catastrophic SE that led to severe neurologic sequelae has been reported in infants with Dravet syndrome (Chipaux et al., 2010; Takayanagi et al., 2010). The catastrophic SE did not seem to be related to a delay in seizure treatment or to insufficient treatment. This SE was always associated with fever and was resistant to conventional SE

treatment, requiring high doses of barbiturates or short-acting barbiturates to control the SE, which may have contributed to cerebral damage resulting from a reduction of cerebral blood flow (Chipaux et al., 2010). Although barbiturates are often chosen to treat refractory SE in the intensive care unit (ICU) setting, it may be beneficial to consider an alternative treatment such as propofol or a combination of hypothermia therapies in these cases (Munakata et al., 2000). The frequency of SE or of prolonged seizures decreases markedly in children with Dravet syndrome who are older than 4 years of age. Therefore, mortality related to acute encephalopathy with SE at this age was an unexpected event for the families of these patients and for the health care professionals (Oguni et al., 2001; Dravet et al., 2005). In Japan, fulminant acute encephalopathy associated with SE in children has recently been identified as a complication of an influenza infection. The individual genetic factors that contribute to the susceptibility to acute encephalopathy may suggest an important role in its pathogenesis (Mizuguchi et al., 2007). For patients with Dravet syndrome, *SCN1A* mutations are related to seizures that are markedly sensitive to elevated temperature. In an *SCN1A*-knockout mouse model, a rise in body temperature markedly decreased the threshold of the seizures; therefore, the complication of acute encephalopathy with SE may be associated with *SCN1A* mutations (Oakley et al., 2009). A previous study indicated that Dravet syndrome was present in most patients who had been diagnosed with vaccine encephalopathy (Berkovic et al., 2006). This disorder frequently causes acute encephalopathy; however, the peak incidence of fatal acute encephalopathy with SE at approximately 6 years of age should be clarified.

All of the patients who had accidental deaths drowned while bathing. Drowning-related mortality is avoidable in patients with Dravet syndrome and in patients with other types of epilepsy (Gaitatzis & Sander, 2004). Because seizures that are hypersensitive to elevated body temperature continue through adulthood in most patients with this disorder, the Japanese-style bathing that raises body temperature is a potential risk factor (Oguni et al., 2001). Therefore, it is necessary to train caregivers to be vigilant when the patients take a bath.

The prevalence of mortality in patients with Dravet syndrome has been shown to range from 5–20%, which is markedly higher than in patients with other types of epilepsy (Oguni et al., 2001; Dravet et al., 2005). In the present study, the statistical analyses involving the 91 hospitals showed a mortality rate of 10.1%. The data from the 26 hospitals that reported mortality cases indicated that the mortality rate was 14.4%. However, a limitation of this study was that the survey period differed among the hospitals, leading to difficulty in accurately evaluating the population (as a denominator). In addition, the lack of detailed information on the population did not permit us to create a survival curve. Other limitations of this study included a 60% response rate to the questionnaire, retrospective case ascertainment, a very low autopsy rate, and a low incidence of *SCN1A* mutation analyses, all of which lowered the validity of this study. However, even if these limitations are considered, the prevalence of early death would be estimated to be 10–15%, which is still markedly higher than the rate in patients with other types of epilepsies.

The mortality rate in childhood epilepsy has been estimated to be 3–7 times higher than that in the general population (Berg et al., 2004; Autry et al., 2010). The risk factors for mortality were considered to be symptomatic etiology, epileptic encephalopathy, especially West and Lennox-Gastaut syndromes, and severe comorbid neurologic disorders. The death rate for the epileptic syndromes was highest for symptomatic generalized epilepsy, which was 15–16% and was almost equivalent to that of Dravet syndrome. However, the causes of death for generalized epilepsy were markedly different from those for Dravet syndrome and were mostly related to the complications of severe neurologic deficits (infections and accidents, among others), not to the occurrences of seizures or sudden death.

In conclusion, this study identifies the high-risk age periods with respect to the specific causes of mortality; however, no other prognostic factors, including *SCN1A* mutations, could be discerned. Since the 1980s, there has been a strong medical/social interest in SUDEP in patients with patients (Nilsson et al., 1999; Gaitatzis & Sander, 2004; Tomson et al., 2008). According to a report that was published by a collaborative special committee of the American Society of Epilepsy and the Foundation of Epilepsy, future endeavors should emphasize the importance of talking with patients' families about SUDEP, facilitating physicians' and community members' understanding of SUDEP, and planning nationwide/international prospective studies (So et al., 2009). It is necessary to provide the information obtained in this nationwide survey regarding the causes of mortality and the high-risk age periods to the hospitals that are involved in the treatment of this disorder and to the patients' families, despite objections that have been raised concerning the difficulty of SUDEP prediction and families' anxiety levels. A worldwide multiinstitutional study needs to be performed to identify the risk factors at a molecular level and to prevent catastrophic events associated with this syndrome.

Acknowledgments

We are grateful to all of the doctors who participated in this nationwide study and who provided clinical data on the patients. This study was funded in part by Research Grants (21210301) for the Specified Disease Treatment Research Program from the Ministry of Health, Labor, and Welfare.

Disclosure

There are no conflicts of interest related to this manuscript. We confirm that we have read the Journal's position regarding issues pertaining to ethical publication and affirm that this report is consistent with those guidelines.

References

Autry AR, Trevathan E, Van Naarden Braun K, Yeargin-Allsopp M. (2010) Increased risk of death among children with Lennox-Gastaut syndrome and infantile spasms. *J Child Neurol* 25:441–447.

Berg AT, Shinnar S, Testa FM, Levy SR, Smith SN, Beckerman B. (2004) Mortality in childhood-onset epilepsy. *Arch Pediatr Adolesc Med* 158:1147–1152.

Berkovic SF, Harkin L, McMahon JM, Pelekanos JT, Zuberi SM, Wirrell EC, Gill DS, Iona X, Mulley JC, Scheffer IE. (2006) De-novo mutations of the sodium channel gene *SCN1A* in alleged vaccine encephalopathy: a retrospective study. *Lancet Neurol* 5:488–492.

Chipaux M, Villeneuve N, Sabouraud P, Desguerre I, Boddaert N, Depienne C, Chiron C, Dulac O, Nabbout R. (2010) Unusual consequences of status epilepticus in Dravet syndrome. *Seizure* 19:190–194.

Claes L, Del-Favero J, Ceulemans B, Lagae L, Van Broeckhoven C, De Jonghe P. (2001) De novo mutations in the sodium-channel gene *SCN1A* cause severe myoclonic epilepsy of infancy. *Am J Hum Genet* 68:1327–1332.

Depienne C, Trouillard O, Saint-Martin C, Gourfinkel-An I, Bouteiller D, Carpentier W, Keren B, Abert B, Gautier A, Baulac S, Arzimanoglou A, Cazeneuve C, Nabbout R, LeGuern E. (2009) Spectrum of *SCN1A* gene mutations associated with Dravet syndrome: analysis of 333 patients. *J Med Genet* 46:183–191.

Dravet C, Bureau M, Oguni H, Fukuyama Y, Cokar O. (2005) Severe myoclonic epilepsy in infancy (Dravet syndrome). In Roger J, Bureau M, Dravet C, Genton P, Tassinari CA, Wolf P (Eds) *Epileptic syndromes in infancy, childhood and adolescence*, 4th ed. John Libbey Eurotext Ltd, London and Paris, pp. 89–113.

Fujiwara T, Sugawara T, Mazaki-Miyazaki E, Takahashi Y, Fukushima K, Watanabe M, Hara K, Morikawa T, Yagi K, Yamakawa K, Inoue Y. (2003) Mutations of sodium channel α subunit type 1 (*SCN1A*) in intractable childhood epilepsies with frequent generalized tonic clonic seizures. *Brain* 126:531–546.

Gaitatzis A, Sander JW. (2004) The mortality of epilepsy revisited. *Epileptic Disord* 6:3–13.

Lossin C. (2009) A catalog of *SCN1A* variants. *Brain Dev* 31:114–130.

Mizuguchi M, Yamanouchi H, Ichiyama T, Shiomi M. (2007) Acute encephalopathy associated with influenza and other viral infections. *Acta Neurol Scand Suppl* 186:45–56.

Munakata M, Kato R, Yokoyama H, Haginoya K, Tanaka Y, Kayaba J, Kato T, Takayanagi R, Endo H, Hasegawa R, Ejima Y, Hoshi K, Iinuma K. (2000) Combined therapy with hypothermia and anticytokine agents in influenza A encephalopathy. *Brain Dev* 22:373–377.

Nilsson L, Farahmand BY, Persson PG, Thiblin I, Tomson T. (1999) Risk factors for sudden unexpected death in epilepsy: a case–control study. *Lancet* 353:888–893.

Oakley JC, Kalume F, Yu FH, Scheuer T, Catterall WA. (2009) Temperature- and age-dependent seizures in a mouse model of severe myoclonic epilepsy in infancy. *Proc Natl Acad Sci U S A* 106:3994–3999.

Ogiwara I, Miyamoto H, Morita N, Atapour N, Mazaki E, Inoue I, Takeuchi T, Itohara S, Yanagawa Y, Obata K, Furuichi T, Hensch TK, Yamakawa K. (2007) Na(v)1.1 localizes to axons of parvalbumin-positive inhibitory interneurons: a circuit basis for epileptic seizures in mice carrying an *Scn1a* gene mutation. *J Neurosci* 27:5903–5914.

Oguni H, Hayashi K, Awaya Y, Fukuyama Y, Osawa M. (2001) Severe myoclonic epilepsy in infants – a review based on the Tokyo Women's Medical University series of 84 cases. *Brain Dev* 23:736–748.

Oguni H, Hayashi K, Osawa M, Awaya Y, Fukuyama Y, Fukuma G, Hirose S, Mitsudome A, Kaneko S. (2005) Severe myoclonic epilepsy in infants. Typical and borderline groups in relation to *SCN1A* mutations. In Delgado-Escueta V, Guerrini R, Medina MT, Genton P, Bureau M, Dravet C (Eds) *Advances in neurology, vol. 95, myoclonic epilepsies*. Lippincott Williams & Wilkins, Philadelphia, pp. 103–117.

So EL, Bainbridge J, Buchhalter JR, Donalty J, Donner EJ, Finucane A, Graves NM, Hirsch LJ, Montouris GD, Temkin NR, Wiebe S, Sierzant TL. (2009) Report of the American Epilepsy Society and the Epilepsy Foundation Joint Task Force on Sudden Unexpected Death in Epilepsy. *Epilepsia* 50:917–922.

Takayanagi M, Haginoya K, Umehara N, Kitamura T, Numata Y, Wakusawa K, Hino-Fukuyo N, Mazaki E, Yamakawa K, Ohura T, Ohtake M. (2010) Acute encephalopathy with a truncation mutation in the *SCN1A* gene: a case report. *Epilepsia* 51:1886–1888.

Tomson T, Nashef L, Ryvlin P. (2008) Sudden unexpected death in epilepsy: current knowledge and future directions. *Lancet Neurol* 7:1021–1031.

Yu FH, Mantegazza M, Westenbroek RE, Robbins CA, Kalume F, Burton KA, Spain WJ, McKnight GS, Scheuer T, Catterall WA. (2006) Reduced sodium current in GABAergic interneurons in a mouse model of severe myoclonic epilepsy in infancy. *Nat Neurosci* 9:1142–1149.

Appendix

The Dravet Syndrome Prognosis Research Group included the following pediatric neurologists who contributed to this study: Hideo Aiba (Shizuoka Children's Hospital), Akashi Ishikawa (Nirenokai Children's Clinic), Yuji Inaba (Shinshu University Hospital), George Imataka (Dokkyo Medical University), Shoichi Endo (Kagawa Children's Hospital), Iori Ohmori (Okayama University), Kyou Kajitani (Kawasaki Hospital), Osamu Kanazawa (Saitama Medical University Hospital), Hisashi Kawawaki (Osaka City Medical Center), Toru Konishi (Nagaoka Rehabilitation Center for Disabled Children), Nobuzo Shimizu (Gunma Institute for Children with Physical Disabilities), Takashi Soga (Epilepsy Center Bethel), Tomoyuki Takano (Shiga University of Medical Science Hospital), Jun Toyama (Nishi-Niigata Chuo National Hospital), Shinichiro Hamano (Saitama Children's Medical Center), Tatsuya Fukasawa (Nagoya University Hospital), Katsuyuki Fukushima (Fukushima Neuro Clinic), Mitsunari Fukuda (Ehime University Hospital), Naomi Fukuyo (Tohoku University Hospital), Hirofumi Fujita (Hirosaki University School of Medicine & Hospital), Shinji Fujimoto (Tsutsujigaoka Children's Clinic), Kimio Minagawa (Hokkaido Medical Center for Child Health and Rehabilitation), Susumu Miyake (Kagawa Prefectural Central Hospital), Nobuko Moriyama (Ibaraki Children's Hospital), and Keiichi Yamamoto (Isehara Kyodo Hospital).

ELSEVIER

Brain & Development 34 (2012) 107–112

BRAIN & DEVELOPMENT
Official Journal of the Japanese Society of Child Neurology

www.elsevier.com/locate/braindev

Case report

A boy with a severe phenotype of succinic semialdehyde dehydrogenase deficiency

Yoko Yamakawa [a,b,*], Tomoyuki Nakazawa [a], Asuka Ishida [a], Nobutomo Saito [a], Mitsutaka Komatsu [a], Tomoyo Matsubara [a], Kaoru Obinata [a], Shinichi Hirose [c], Akihisa Okumura [b], Toshiaki Shimizu [b]

[a] *Department of Pediatrics, Juntendo University, Urayasu Hospital, Japan*
[b] *Department of Pediatrics, Juntendo University, School of Medicine, Japan*
[c] *Department of Pediatrics, Fukuoka University, School of Medicine, Japan*

Received 20 December 2010; received in revised form 4 May 2011; accepted 6 May 2011

Abstract

Succinic semialdehyde dehydrogenase (SSADH) deficiency is a rare autosomal recessive disorder affecting γ-aminobutyric acid degradation. We describe here a boy with a severe phenotype of SSADH deficiency. He was referred because of a developmental delay at 4 months of age. At the age of 8 months, severe seizures developed. The diagnosis of SSADH deficiency was confirmed by an increase in 4-hydroxybutyric acid and heteroallelic mutation in the *ALDH5A1* gene. His seizures were successfully treated with high-dose phenobarbital, and the electroencephalogram (EEG) abnormalities were ameliorated. However, the patient showed a degenerative clinical course with severe neurological deficits. A magnetic resonance imaging (MRI) scan revealed abnormal high intensities in the putamina and caudate nuclei on T2-weighted images, followed by marked atrophic changes. The clinical manifestation of our patient indicates the wide variety of SSADH deficiency phenotypes.

1. Introduction

Succinic semialdehyde dehydrogenase (SSADH) deficiency is a rare autosomal recessive disorder affecting the degradation of γ-aminobutyric acid (GABA). SSADH works with GABA transaminase to converts GABA to succinate. In the absence of SSADH, GABA is not broken down into succinic acid, but is converted into γ-hydroxybutyric acid (GHB). It is unclear whether elevated GABA, GHB, or another neurometabolic change accounts for the phenotype, but the primary metabolic abnormality is an excessive concentration of GHB in the physiological fluids, with elevations up to 800-fold in the plasma and 1200-fold in the cerebrospinal fluid [1]. The SSADH gene (*ALDH5A1*) has been mapped to chromosome 6p22. More than 350 patients with SSADH deficiency have been identified worldwide. In Japan, Ishiguro et al. [2] reported the first patient in 2001, and since then, only a few patients have been reported.

SSADH deficiency often presents in childhood with non-specific clinical manifestations. The most common neurological symptoms include language delay, ataxia, hypotonia, and mental retardation. Seizures are less common, occurring in about half of all patients [3]. Although SSADH deficiency does not generally manifest as a degenerative condition, developmental regres-

* Corresponding author. Address: Department of Pediatrics, Juntendo University, School of Medicine, 2-1-1 Hongo, Bunkyo-ku, Tokyo 113-8421, Japan. Tel.: +81 3 3813 3111; fax: +81 3 5800 1580.
E-mail address: yooyoo@juntendo.ac.jp (Y. Yamakawa).

0387-7604/$ - see front matter © 2011 The Japanese Society of Child Neurology. Published by Elsevier B.V. All rights reserved.
doi:10.1016/j.braindev.2011.05.003

sion has been occasionally reported. Moreover, some patients may have a more fulminant clinical course, with the early onset of clinical symptoms, seizures, choreoathetosis, myoclonus, and optic atrophy, resulting in death in infancy [3].

We describe here a boy with SSADH deficiency who had a severe phenotype with severe seizures, marked neuroimaging abnormalities, and a degenerative clinical course. His seizures were successfully treated using high-dose phenobarbital (PB). We also describe the magnetic resonance imaging (MRI) and amplitude-integrated electroencephalogram (aEEG) findings for this patient.

2. Patient report

A 4-month-old boy was referred to our hospital for an evaluation of developmental delay. He was the third child of non-consanguineous healthy parents. His elder sisters were healthy and had achieved normal development. On the first presentation, the patient's visual tracking and head control were insufficient. Neurological examination revealed generalized hypotonia with normal deep tendon reflexes. No external anomaly was observed. Blood tests including blood gas analysis, blood chemistry, thyroid function, lactic and pyruvic acids, and karyotypic chromosome analysis were unremarkable. No abnormal findings were seen in the cranial MRI or EEG.

The patient had had repetitive aspiration pneumonia since the age of 7 months. He was diagnosed as having gastro-esophageal reflux on the basis of 24-h pH monitoring and a barium esophagram. He required an esophagoduodenal tube to prevent aspiration pneumonia. A deterioration in psychomotor development was noted when the patient was 8 months old, along with the development of intractable seizures. The diagnosis of SSADH deficiency was made on the basis of urine organic acid analysis using gas chromatography–mass spectrometry. A marked increase in 4-hydroxybutyric acid, which is crucial for the diagnosis of SSADH deficiency, was found. Analysis of the *ALDH5A1* gene encoding SSADH revealed compound heterozygous mutations with c. 366 del G (W112fsX112) and c.1294 A > C (M432L).

The patient's seizures were characterized by loss of consciousness followed by clonic convulsion of the left upper and lower extremities lasting for several minutes. Carbamazepine, zonisamide, and vitamin B6 were ineffective in controlling the seizures. Although continuous infusion of midazolam was effective, the seizures recurred. High-dose PB treatment was started at 10 months of age. PB in a dose of 20 mg/kg/day was given rectally for the first two days and then orally in a dose of 10 mg/kg/day from the third day. The patient's seizures were controlled after the initiation of high-dose PB treatment, and the midazolam infusion was discontinued. The EEG conducted prior to the administration of high-dose PB showed markedly disorganized background activity and frequent high-voltage slow waves, sharp waves, and spikes (Fig. 1). However, after the high-dose PB treatment, the frequency and voltage of the sharp waves and spikes were significantly reduced, and no high-voltage slow waves were observed (Fig. 1).

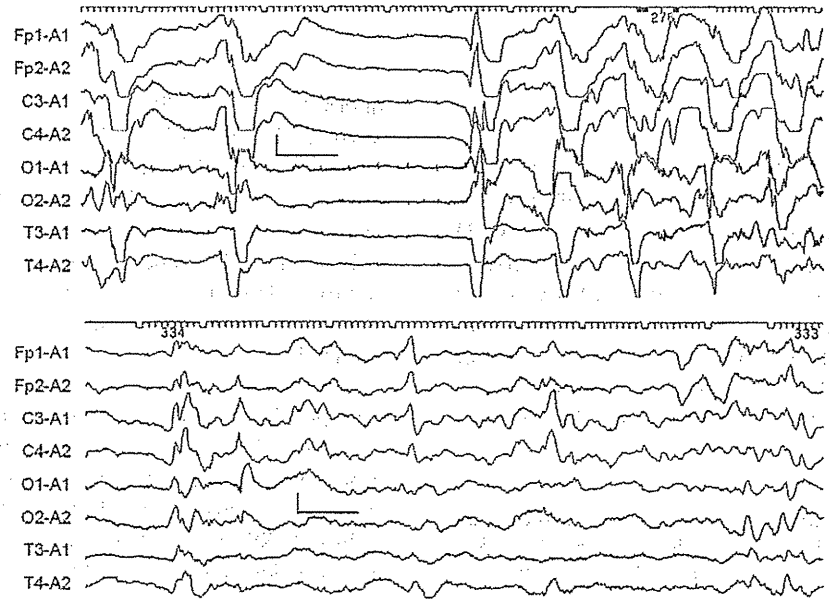

Fig. 1. Conventional EEG. Top: EEG before high-dose phenobarbital treatment. Markedly disorganized background EEG activity and frequent appearance of high-voltage slow waves, sharp waves, and spikes were observed. Bottom: EEG after high-dose phenobarbital treatment. The frequency and voltage of the sharp waves and spikes were markedly reduced. High-voltage slow waves were not present. Calibration, 100 μV, 1 s.

Single-channel aEEG (CFM-6000, Olympic Medical, Seattle, WA, USA) was performed for 353 h to monitor the efficacy of antiepileptic drugs. We used the Fp1–Fp2 rather than the P3–P4 derivation usually used in neonates because the patient's hair interfered with stable long-term electrode placement in the parietal area. The upper border of the aEEG trace was continuously greater than 50 μV before the administration of PB (Fig. 2). The raw EEG data showed frequent high-voltage sharp waves and spikes, and seizures were also visible on the aEEG (Fig. 2). In this patient, the seizures observed on the aEEG were always accompanied by clinical manifestations such as convulsive movement. Administration of high-dose PB decreased the upper border of the aEEG trace to 25–50 μV. No seizures were observed on the EEG after the initiation of high-dose PB.

The head MRI at 4 months of age was unremarkable (Fig. 3). However, at 8 months of age, the MRI scan revealed abnormally high intensities in the caudate nuclei and putamina associated with mild enlargement of the extra-axial space on T2-weighted images (Fig. 3). The MRI at 17 months of age revealed severe atrophy of the caudate nuclei, high intensities in the

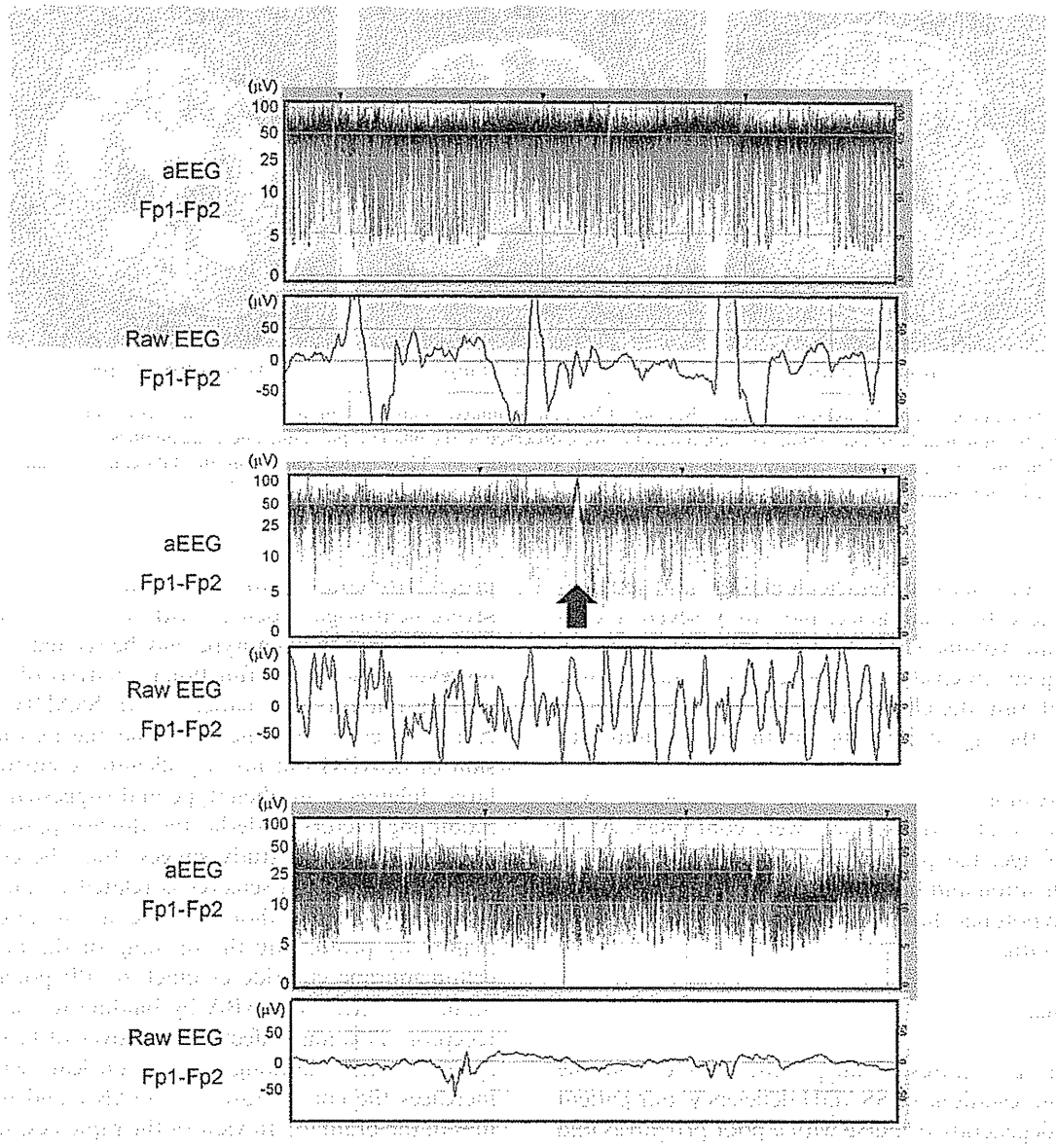

Fig. 2. Amplitude-integrated EEG. Top: Amplitude-integrated EEG (aEEG) before high-dose phenobarbital treatment. The upper border of the aEEG trace was constantly beyond 50 μV. This indicates that high amplitude EEG activities were present throughout aEEG recording. The raw EEG also showed frequent appearance of high-voltage sharp waves and spikes. Middle: A seizure detected on the aEEG. A transient rise in the lower border suggested ictal EEG changes (arrow). Ictal EEG changes were confirmed by the raw EEG showing repetitive and rhythmic sharp waves during the same period. Bottom: The aEEG after high-dose phenobarbital treatment. The upper border of the aEEG trace was 25–50 μV. This indicated the reduction in amplitude of background EEG activities. The raw EEG also demonstrated sporadic appearance of paroxysmal discharges with reduced amplitude.

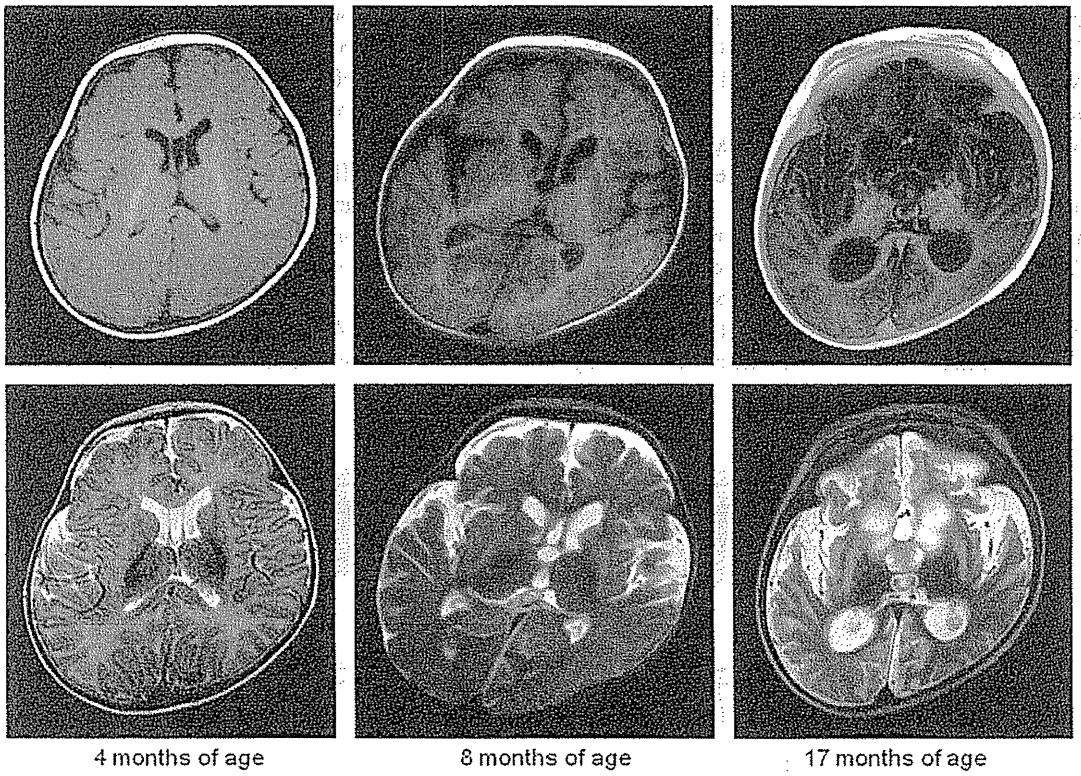

Figure 3. MRI findings. Top: T1-weighted images, Bottom: T2-weighted images. Left: at 4 months of age, no remarkable abnormalities were observed. Middle: at 8 months of age, abnormal high intensities were observed in the bilateral putamina and caudate nuclei on T2-weighted images. Right: at 17 months of age, severe caudate nuclei atrophy, high intensities on T2-weighted images in the bilateral putamina, and marked ventriculomegaly and enlargement of extra-axial space were seen.

putamina, and marked ventriculomegaly and enlargement of the extra-axial space, indicating severe reduction of brain volume (Fig. 3). No significant alteration in the signal intensity of the globus pallidus was observed during the clinical course, and no atrophy or change in the signal intensity of the cerebellum was found.

A regression in psychomotor development was observed even after the seizures were controlled. At 23 months of age, the patient remained bed-ridden, with poor eye fixation and head control and remarkable generalized hypotonia, however, seizures did no occur for several months.

3. Discussion

The clinical features of our patient differed from the typical manifestations of SSADH deficiency: our patient showed a degenerative course with a poor prognosis and had MRI lesions in the putamina and caudate nuclei, together with severe atrophy of the cerebrum and severe EEG abnormalities.

SSADH deficiency is typically a slowly progressive or static encephalopathy with late infantile to early childhood onset [4]. In contrast, our patient had an obvious progressive course with mid-infantile onset resulting in severe neurological deficits with marked brain atrophy. The difference in phenotype may be related to genotype; however, following a functional analysis of 27 disease-causing mutations in patients with SSADH deficiency, Akaboshi et al. [5] concluded that the residual expression of SSADH did not significantly contribute to the large differences in phenotype and suggested that other modifying factors underlie the disease pathology. The results of our case study suggest that the effectiveness of high-dose PB on seizures is related to the difference in phenotype. PB is thought to act as an anticonvulsant mainly by prolonging the opening of the postsynaptic cell-membrane chloride channel [6]. PB potentiates the inhibitory effect of GABA by binding to the GABA-A receptor. This may affect the turnover of GABA in the synaptic cleft, although it is unclear whether PB increases the concentration of GABA and its metabolites in the brain [6]. In view of the rapid cessation of seizures, we conclude that the PB treatment was beneficial to our patient.

The characteristic neuroimaging abnormalities in patients with SSADH deficiency include increased signal intensity in the globus pallidus, subcortical white matter, cerebellar dentate nucleus, and brainstem on T2-

weighted images [7]. Other neuroimaging abnormalities are cerebral atrophy, delayed myelination, and a pattern of dentate-pallidal hyperintensity [8,9]. The putamina and caudate nuclei were predominantly involved in our patient, whereas the globus pallidus and cerebellar dentate nuclei were almost completely spared. In our patient, homogeneous hyperintensity was observed in the putamina at 8 and 17 months of age. The caudate nuclei showed increased T2 signals at 8 months of age and marked atrophy at 17 months of age. To our knowledge, no reports have described this pattern of lesions on MRI scans in patients with SSADH deficiency. Pearl et al. [10] reported that MRI scans showed predominant changes in the thalamus and basal ganglia of epileptic infants treated with a relatively high dose of vigabatrin, an irreversible GABA transaminase inhibitor, suggesting that this treatment may also affect brain lesions in children with SSADH deficiency.

Epilepsy is present in nearly half of the patients with SSADH deficiency [4]. EEG abnormalities in patients with SSADH deficiency include generalized and focal epileptiform discharges, photosensitivity, background slowing, and sleep spindle asynchrony [4]. Compared with children who have a typical SSADH deficiency, our patient had more frequent seizures and more severe abnormalities in background EEG activity, with frequent epileptiform discharges. No standard therapy for SSADH deficiency exists, although vigabatrin is considered to be a logical choice because it inhibits the conversion of GABA–GHB [11]. However, the laboratory and clinical reports of the effect of vigabatrin have been inconsistent [12]. Moreover, vigabatrin is not currently available in Japan; thus, we administered PB to control severe seizures in our patient. Although PB effectively stopped the seizures in our patient, its effects on the clinical course of SSADH are unclear. Further studies are necessary to clarify the optimal treatment for SSADH deficiency.

The continuous EEG monitoring of our patient using aEEG was useful because aEEG monitoring can show seizure burden objectively and quantitatively. Precise evaluation of the seizure burden is difficult using direct observation because the clinical symptoms of seizures in children can be subtle and may be overlooked. Ishikawa et al. performed aEEG monitoring combined with conventional EEG during clusters of seizures in a child with frontal lobe epilepsy [13]. A total of 197 seizures were recorded during the first 24 h and the decrease and disappearance of seizures were confirmed using aEEG monitoring. Stewart et al. evaluated the diagnostic accuracy of color density spectral array and aEEG for seizure identification in the intensive care unit [14]. The median sensitivity for seizure identification was 83.3% using color density spectral array and 81.5% using aEEG. These results suggest usefulness of aEEG for seizure identification. In addition, aEEG monitoring showed the changes in background EEG activity, revealing the efficacy of the antiepileptic treatment in our patient. The lower border of the aEEG trace was markedly reduced after administration of high-dose PB, indicating that the EEG abnormalities were ameliorated. These findings suggest that aEEG is useful for monitoring the effect of treatment in children with frequent seizures and/or severe EEG abnormalities as well as in children with acute encephalopathy [15].

In summary, the present paper presents the case of a boy with a severe phenotype of SSADH deficiency characterized by obviously progressive clinical course with severe neurological deficits. His clinical features included a degenerative course, characteristic MRI lesions in the putamina and caudate nuclei, which has not been previously reported in patients with SSADH, and seizures that were controlled by PB administration. The clinical manifestations of our patient indicate the wide variety of SSADH deficiency phenotypes.

Acknowledgments

We would like to thank Dr. Masaki Takayanagi and Dr. Kei Murayama from the Department of Metabolism, Chiba Children's Hospital for their useful advice.

References

[1] Gibson KM, Aramaki S, Sweetman L, Nyhan WL, DeVivo DC, Hodson AK, et al. Stable isotope dilution analysis of 4-hydroxybutyric acid: an accurate method for quantification in physiological fluids and the prenatal diagnosis of 4-hydroxybutyric aciduria. Biomed Environ Mass Spectrom 1990;19:89–93.
[2] Ishiguro Y, Kajita M, Aoshima T, Watanabe K, Kimura M, Yamaguchi S. The first case of 4-hydroxybutyric aciduria in Japan. Brain Dev 2001;23:128–30.
[3] Rahbeeni Z, Ozand PT, Rashed M, Gascon GG, Nasser M, Odaib A, et al. 4-Hydroxybutyric aciduria. Brain Dev 1994;16:64–71.
[4] Pearl PL, Gibson KM, Acosta MT, Vezina LG, Theodore WH, Rogawski MA, et al. Clinical spectrum of succinic semialdehyde dehydrogenase deficiency. Neurology 2003;60:1413–7.
[5] Akaboshi S, Hogema BM, Novelletto A, Malaspina P, Salomons GS, Maropoulos GD, et al. Mutational spectrum of the succinate semialdehyde dehydrogenase (ALDH5A1) gene and functional analysis of 27 novel disease-causing mutations in patients with SSADH deficiency. Hum Mutat 2003;22:442–50.
[6] Barker JL, McBurney RN. Phenobarbitone modulation of postsynaptic GABA receptor function on cultured mammalian neurons. Proc R Soc Lond B Biol Sci 1979;206:319–27.
[7] Pearl PL, Jakobs C, Gibson KM. Disorders of beta- and gamma-amino acids in free and peptide-linked forms. In: Scrive CR et al., editors. Online molecular and metabolic bases of inherited disease, chapter 91, online: http://www.ommbid.com.
[8] Yalçinkaya C, Gibson KM, Gündüz E, Koçer N, Fiçicioğlu C, Küçükercan I. MRI findings in succinic semialdehyde dehydrogenase deficiency. Neuropediatrics 2000;31:45–6.
[9] Ziyeh S, Berlis A, Korinthenberg R, Spreer J, Schumacher M. Selective involvement of the globus pallidus and dentate nucleus

in succinic semialdehyde dehydrogenase deficiency. Pediatr Radiol 2002;32:598–600.
[10] Pearl PL, Vezina LG, Saneto RP, McCarter R, Molloy-Wells E, Heffron A, et al. Cerebral MRI abnormalities associated with vigabatrin therapy. Epilepsia 2009;50:184–94.
[11] Pearl PL, Gibson KM, Cortez MA, Wu Y, Carter Snead O, Knerr I, et al. Succinic semialdehyde dehydrogenase deficiency: lessons from mice and men. J Inherit Metab Dis 2009;32:343–52.
[12] Gibson KM, Christensen E, Jakobs C, Fowler B, Clarke MA, Hammersen G, et al. The clinical phenotype of succinic semialdehyde dehydrogenase deficiency (4-hydroxybutyric aciduria): case reports of 23 new patients. Pediatrics 1997;99:567–74.
[13] Ishikawa N, Kobayashi Y, Kobayashi M. A case of frontal lobe epilepsy in which amplitude-integrated EEG combined with conventional EEG was useful for evaluating clusters of seizures. Epilepsy Behav 2010;18:485–7.
[14] Stewart CP, Otsubo H, Ochi A, Sharma R, Hutchison JS, Hahn CD. Seizure identification in the ICU using quantitative EEG displays. Neurology 2010;75:1501–8.
[15] Komatsu M, Okumura A, Matsui K, Kitamura T, Sato T, Shimizu T, et al. Clustered subclinical seizures in a patient with acute encephalopathy with biphasic seizures and late reduced diffusion. Brain Dev 2010;32:472–6.

available at www.sciencedirect.com

ScienceDirect

www.elsevier.com/locate/brainres

BRAIN RESEARCH

Research Report

The developmental changes of $Na_v1.1$ and $Na_v1.2$ expression in the human hippocampus and temporal lobe

Wenze Wang[a,b], *Sachio Takashima*[c], *Yoshie Segawa*[a,d], *Masayuki Itoh*[e], *Xiuyu Shi*[a], *Su-Kyeong Hwang*[a], *Kazuki Nabeshima*[d], *Morishige Takeshita*[d], *Shinichi Hirose*[a,*]

[a]*Department of Pediatrics, School of Medicine, Fukuoka University, Fukuoka, Japan*
[b]*Department of Pathology, Peking Union Medical College Hospital, Chinese Academy of Medical Science, Beijing, PR China*
[c]*Yanagawa Institute for Developmental Disabilities, International University of Health and Welfare, Fukuoka, Japan*
[d]*Department of Pathology, School of Medicine, Fukuoka University, Fukuoka, Japan*
[e]*National Institute of Neuroscience, National Center of Neurology and Psychiatry, Tokyo, Japan*

ARTICLE INFO

Article history:
Accepted 25 February 2011
Available online 4 March 2011

Keywords:
Voltage-gated sodium channel
$Na_v1.1$
$Na_v1.2$
Brain development
Double-staining
immunohistochemistry

ABSTRACT

Alterations of the genes encoding α1 and α2 subunits of voltage-gated sodium channels (SCN1A, SCN2A) have been reported as causes of various types of epilepsy, most of which occur during the first year of life; as yet, however, the detailed mechanisms are unclear. We suppose that developmental changes of SCN1A and SCN2A in the human brain, which are unknown yet, may play an important role. So here, we studied the developmental changes of their corresponding proteins ($Na_v1.1$ and $Na_v1.2$) in the human hippocampus and temporal lobe in 28 autopsy cases, which age from 13 weeks of gestation (GW) to 63 years of age (Y). Using comparative microscopic immunohistochemical (IHC) analysis, we found that $Na_v1.1$ and $Na_v1.2$ immunoreactivity first appeared at 19GW, simultaneously in the hippocampus and the white matter of temporal lobe. In nearly all age groups, $Na_v1.1$ immunoreactivity was weak and relatively homogeneous. In general, $Na_v1.1$ immunoreactive (IR) neurons and neurites increased during the late fetal and postnatal periods, reached their peaks 7–9 months after birth (M), then decreased and remained stable at a relatively low level during childhood and adulthood. On the other hand, $Na_v1.2$ immunoreactivity was strong and heterogeneous. In the hippocampus, $Na_v1.2$ IR neurons increased gradually during the late fetal period, reached their peaks at 7–9M, sustained this high level during childhood, and then decreased slightly at adulthood. In the temporal lobe, $Na_v1.2$ IR neurons reached a high level during the late fetal period, and maintained that level during subsequent developmental stages; $Na_v1.2$ IR neurites also increased to a relatively high level during the late fetal period and continued to increase up to and during adulthood. Using double-staining IHC, we found that $Na_v1.1$ and $Na_v1.2$ had a relatively high colocalization rate with parvalbumin and showed distinct developmental changes. These findings extend our previous understanding of sodium channels and may help us discover the pathomechanisms of sodium channel-related age-dependent epilepsy.

* *Corresponding author at:* Department of Pediatrics, School of Medicine, Fukuoka University, 45–1, 7-chome Nanakuma, Jonanku, Fukuoka 814–0180, Japan. Fax: +81 92 862 6955.
E-mail address: hirose@fukuoka-u.ac.jp (S. Hirose).

0006-8993/$ – see front matter © 2011 Elsevier B.V. All rights reserved.
doi:10.1016/j.brainres.2011.02.083

1. Introduction

Voltage-gated sodium channels play an important role in neuronal excitability and are significant therapeutic targets in epilepsy, pain and local anesthesia, and are currently under investigation for stroke, bipolar disorder, and other disorders (Clare et al., 2000). Our previous and other related studies have proven that abnormalities of the genes encoding α1 and α2 subunits of voltage-gated sodium channels (SCN1A, SCN2A) are associated with a variety of epilepsies: Dravet syndrome; intractable childhood epilepsy with generalized tonic–clonic seizures (ICEGTC); generalized epilepsy with febrile seizures plus (GEFS+); and some other rare early onset epileptic encephalopathies, most of which usually occur in the first year of life (Fukuma et al., 2004; Kumakura et al., 2009; Shi et al., 2009; Sugawara et al., 2001; Wang et al., 2008). Still, how these sodium channels cause these age-dependent onset epilepsies is unclear. In animal brains, there have been many reports of the expression and developmental changes of SCN1A and SCN2A's corresponding proteins ($Na_v1.1$ and $Na_v1.2$), and these have indicated some possible correlation between the expression, developmental changes, and onset of epileptic symptoms (Liao et al., 2010; Ogiwara et al., 2007; Vacher et al., 2008). For the human brain, however, there are few studies and these contain only adults and do not include developmental changes (Lu et al., 1992; Whitaker et al., 2000, 2001a, 2001b).

Recent mouse model studies show that the impairment of interneuron sodium channel activity contributes to seizure generation (Martin et al., 2010; Oakley et al., 2009; Ogiwara et al., 2007; Tang et al., 2009; Yu et al., 2006). Among those, Ogiwara shows that "$Na_v1.1$ is clustered predominantly at the axon initial segments of parvalbumin-positive interneurons" (Ogiwara et al., 2007), indicating that such a colocalization pattern may play an important role in the pathogenesis of epilepsy. There are reports of similar colocalization pattern in rats (Kaneko and Watanabe, 2007; Van Wart et al., 2007). This pattern, however, has not been reported in the human brain. Such information, including the developmental changes, are important not only for a basic understanding of $Na_v1.1$ and $Na_v1.2$'s functions in the human CNS but also for further insight into their roles in different human disease states, especially in age-dependent epilepsies.

The hippocampus and the temporal lobe are considered as the most important regions for seizure generation and are the focus of current epilepsy research. In this report, using comparative microscopic IHC analysis, we studied the developmental changes of $Na_v1.1$ and $Na_v1.2$ expression, and their colocalization with parvalbumin in the human hippocampus and temporal lobe.

2. Results

2.1. *Mono-staining IHC*

2.1.1. *Distribution and developmental changes of $Na_v1.1$ immunoreactivity*

$Na_v1.1$ IR neurons first appeared at 19GW, simultaneously in the hippocampus and the white matter of the temporal lobe. The immunoreactivity was found solely in the nucleus of neurons, and avoided from the cytoplasm and the neuropil. At 22GW, few short IR neurites first appeared in the Cornu Ammonis of the hippocampus, connecting with IR neuronal somata. At 27GW, such neurites could be found in each sub-region of the hippocampus and the temporal lobe. Simultaneously, the IR segment of neurites was longer and more delicate than before. Since then, $Na_v1.1$ IR signals were detected in both neuronal somata and neurites in various shapes, while nuclei avoided. After that, there were no obvious changes in cellular distribution.

In the hippocampus, $Na_v1.1$ IR neurons appeared simultaneously in the Cornu Ammonis (CA) and the Dentate Gyrus (DG), increased gradually and reached their peaks 7–9 months after birth (M), since then decreased and remained relatively low level during childhood and adulthood (Fig. 1). The pyramidal neurons of CA showed denser immunoreactivity than the granular neurons of DG, and showed relatively obvious developmental changes. The $Na_v1.1$ IR neurites scattered in the hippocampus, in various lengths and directions, and showed developmental changes similar to the neurons.

In the white matter of the temporal lobe, $Na_v1.1$ IR neurons first appeared at 19GW, and then remained at this level during the subsequent developmental stages. Those IR neurons were in various shapes, such as oval, pyramidal and spindle shapes, and showed obvious immunoreactivity in their neurites (Fig. 2). In the cortex of the temporal lobe, $Na_v1.1$ IR neurons appeared in each layer by 27GW, increased gradually during late fetal period and reached their peaks at 7–9M, then decreased and sustained a relatively low level during childhood and adulthood. In nearly all age groups, the granular neurons in layer IV showed much denser immunoreactivity than other layers. In the cortex, $Na_v1.1$ IR neurites showed nearly similar developmental changes to the neurons, without obvious decrease (Table 1). These neurites were sparse, delicate and in various lengths, scattered in each sub-region of the temporal lobe. There was no obvious immunoreactivity in neuropil (the background was clean) or fiber tracts.

2.1.2. *Distribution and developmental changes of $Na_v1.2$ immunoreactivity*

$Na_v1.2$ IR neurons first appeared at 19GW, simultaneously in the hippocampus and the temporal lobe. The IR signals were mainly in the nuclei of neurons, and mildly in the neuropil. At 27GW, $Na_v1.2$ IR neurons appeared in each sub-region of the hippocampus and the temporal lobe. Although the neuropil immunoreactivity was strong, we could recognize the dense IR neuronal somata and neurites, while the nuclei usually avoided. After that, there were no obvious changes in cellular distribution.

In the hippocampus, $Na_v1.2$ IR neurons and neurites first appeared at 19GW, simultaneously in the CA and DG, increased gradually with gestational and postnatal age, peaked at 7–9M and sustained such level during childhood. Then the IR neurons slightly decreased to relatively low adult level; the IR neurites sustained that high level during adulthood (Fig. 1). The pyramidal neurons in CA showed much denser immunoreactivity than the granular neurons in DG; while the neuropil in CA showed much weaker immunoreactivity than those in DG.

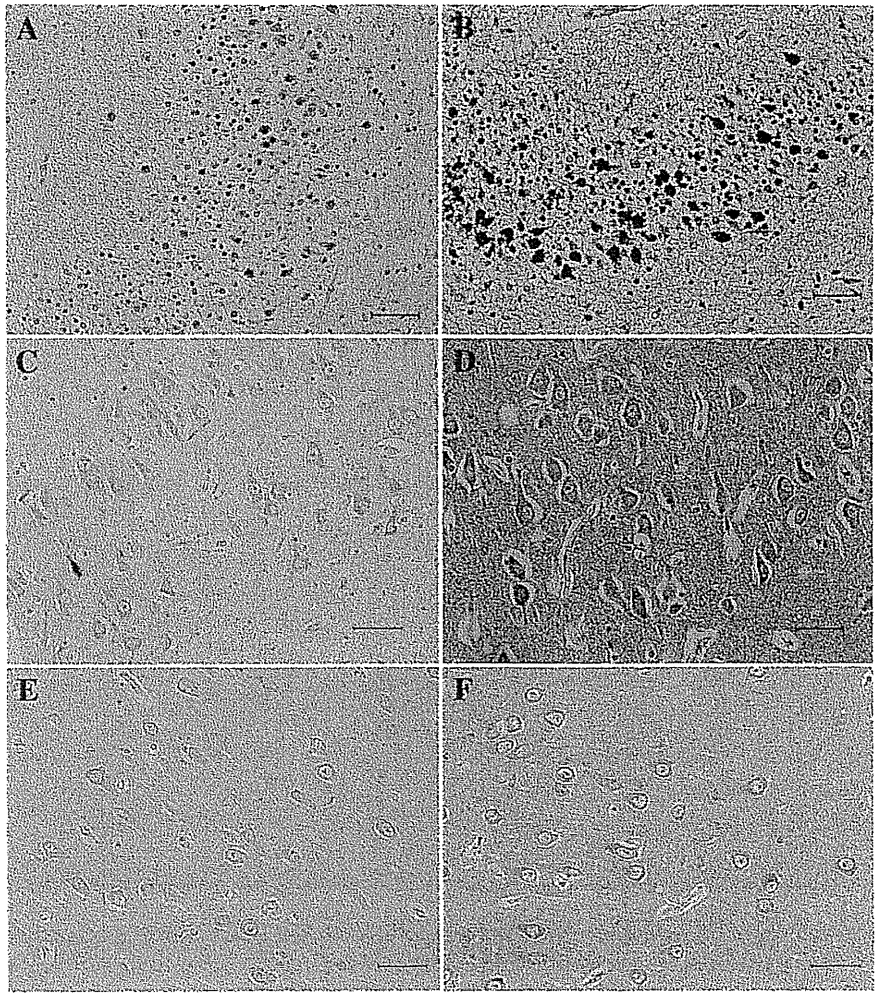

Fig. 1 – Developmental changes of $Na_v1.1$ and $Na_v1.2$ in the hippocampus. A and B from one 22GW fetus case. C and D from one 7M infant case. E and F from one adult case. Left column, $Na_v1.1$ immunoreactivity; right column, $Na_v1.2$ immunoreactivity. Bar, 50 μm. $Na_v1.1$ immunoreactivity is weak, increases with fetal age, reaches the peak at 7M and then decreases to relatively low adult level. $Na_v1.2$ immunoreactivity is strong, especially in the neuropil. It increases with age and only decreases slightly during adulthood.

In the temporal lobe, $Na_v1.2$ IR neurons first appeared simultaneously in the cortex and the white matter at midgestation, increased with fetal age, reached their peaks before birth for nearly all sub-regions and remained at that level. Nearly in all age groups, the pyramidal neurons in layer III and layer V showed much denser immunoreactivity than the granular neurons in layer II and layer IV. Interestingly, the IR pyramidal neurons were continuous from the CA of the hippocampus to layer V of the temporal lobe. $Na_v1.2$ IR neurites increased gradually during the entire human developmental stages, reached their peaks at different stages for different layers respectively, and remained at those levels since then.

2.2. *Double-staining IHC*

2.2.1. *Distribution and developmental changes of $Na_v1.1$ and parvalbumin double-staining*

$Na_v1.1$ and parvalbumin double-stained neurons were first detected since 22GW, simultaneously in the hippocampus and white matter of the temporal lobe. In the hippocampus, the most double-stained neurons were in the CA area, the colocalization rate was 49.8% (105/211), and relatively obvious in the CA3 sub-region. In the white matter of the temporal lobe, the colocalization rate was 65.6% (21/32). Before 27GW, in the double-stained neurons, $Na_v1.1$ IR signals were denser in the periphery while parvalbumin was denser in the central part of the neurons. Before birth, double stained neurons could be detected in the cortex of the temporal lobe. By 2M, the double stained neurons turned into a relatively homogenous "purple color", representing that the immunoreactive signals mixed more uniformly. In the CA area of the hippocampus, the colocalization rate increased gradually, and the CA1 sub-region became more obvious than the CA3. At 7M, the colocalization rate in the CA area of the hippocampus increased to 80.3% (61/76). In the white matter of the temporal lobe, the colocalization rate decreased and couldn't detect double-stained neurons after 2M. In the cortex of the temporal lobe, the double-stained neurons were predominant in layer IV—only few double-stained neurons scattered in other layers,

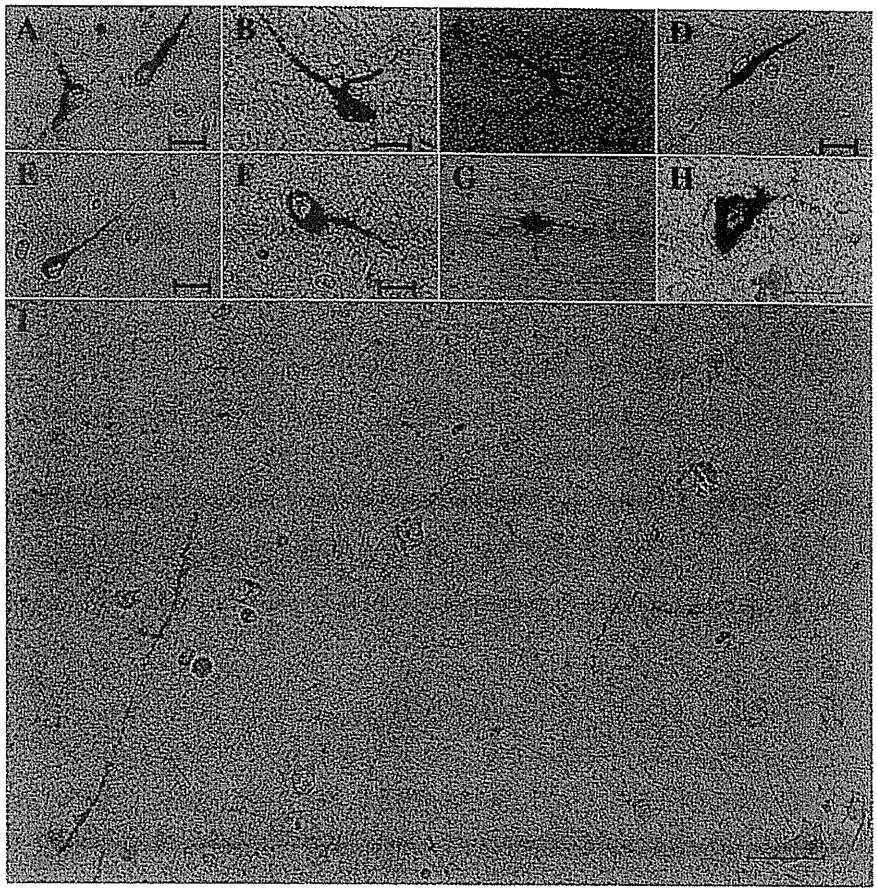

Fig. 2 – $Na_v1.1$ immunoreactivity in the white matter of the temporal lobe. A–H, $Na_v1.1$ immunoreactivity in various shapes of neurons. Both the somata and neurites are positive, while nuclei avoided. I, $Na_v1.1$ immunoreactive delicate neurites are dispersed, in different lengths and directions. Bar: A–F, 10 μm; G, H, 20 μm; I, 50 μm.

so we only counted them in layer IV. The colocalization rate in layer IV increased gradually and reached 98.6% (72/73) at 7M (Fig. 3). Since then, the colocalization rate in the hippocampus and temporal lobe sustained such level during childhood and adulthood (Table 3).

2.2.2. *Distribution and developmental changes of $Na_v1.2$ and parvalbumin double-staining*

$Na_v1.2$ and parvalbumin double-stained neurons were also first detected at 22GW, simultaneously in the CA area of the hippocampus and the white matter of the temporal lobe. In the CA area of the hippocampus, the colocalization rate was 81.5% (154/189), relatively obvious in the CA3 sub-region; in the white matter of the temporal lobe, the colocalization rate was 75.0% (51/68) (Fig. 3). Before 27GW, in the double-stained neurons, $Na_v1.2$ IR signals were denser in the periphery while parvalbumin was denser in the central part of the neurons. Before birth, the colocalization could be detected in the cortex of the temporal lobe. By 2M, the double stained neurons turned into a relatively homogenous "purple color". In the CA area of the hippocampus, the colocalization rate remained relatively stable, while the CA1 sub-region became more obvious, instead of the CA3. At 7M, in the CA area of the hippocampus, the colocalization rate was 80.4% (189/235). In the white matter of the temporal lobe, the colocalization rate decreased and couldn't detect double-stained neurons since 2M. In the cortex of the temporal lobe, the overwhelming majority of double-stained neurons were in the layer IV. At 7M, the colocalization rate in layer IV reached 98.1% (153/156). Since then, the colocalization rate in hippocampus and temporal lobe sustained such level during childhood and adulthood (Table 4).

3. Discussion

Our analysis of the sub-regional and cellular distribution of $Na_v1.1$ and $Na_v1.2$ in the human hippocampus and temporal lobe extends previous understanding by demonstrating the developmental changes of $Na_v1.1$ and $Na_v1.2$ and their colocalization with parvalbumin.

Here, for the first time, the developmental changes of $Na_v1.1$ and $Na_v1.2$ in the human brain were described. In cellular distribution, $Na_v1.1$ and $Na_v1.2$ IR signals immigrated from the nucleus to the cytoplasm and the neurites during fetal development. In sub-regional distribution, $Na_v1.1$ and $Na_v1.2$ IR signals also showed distinct developmental changes (Tables 1 and 2). In the hippocampus and the temporal lobe, $Na_v1.1$ immunoreactivity was weak and relatively homogeneous in all age groups. $Na_v1.1$ IR neurons appeared in midgestation, increased with gestational and postnatal ages,

Table 1 – The microscopic analysis results of $Na_v1.1$ immunostaining in the hippocampus and temporal lobe.

Age group	Hippocampus				Temporal cortex (layer)										Temporal white matter	
	Cornu ammonis		Dentate gyrus		I		II		III		IV		V		VI		
	Neuron	Neurite	Neuron	Neurite	Neuron	Neurite	Neuron	Neurite	Neuron	Neurite	Neuron	Neurite	Neuron	Neurite	Neuron	Neurite	Neuron[a]	Neurite
13GW–17GW	–	–	–	–	–	–	–	–	–	–	x	x	x	x	x	x	–	–
19GW–22GW	+	–	+	–	–	–	±	+	±	–	±	+	x	x	x	x	+	–
27GW–39GW	+1/2	+	+	+	+	+	+	+	+	+	+	+	+	+	+	+	+	+
P1D–1M	++	+	+	+	++	+	+	++	+	++	+	+	+	++	+	++	+	++
1M–2M	++	+	+	+	++	+	+	++	+	++	+	++	+	++	+	++	+	++
7M–9M	+++	++	++	++	++	++	++	+++	++	++	++	+++	++	++	+++	++	+	+++
1Y–5Y	+	+	+	+	++	++	+	++	+	++	++	++	+	++	+	++	+	++
46Y–63Y	+	+	+	+1/2	++	++	+	++	+	++	++	++	+	++	+	++	+	++

x, no such recognizable layer.
[a] The scattered neurons in white matter.

peaked at 7–9M, and then first decreased and stabilized during childhood and adulthood. On the other hand, $Na_v1.2$ immunoreactivity was strong, heterogeneous and diffusely dense in the neuropil, providing a strong "background". In the hippocampus, $Na_v1.2$ IR neurons increased gradually from the late fetal period, peaked at 7–9M, sustained their high level during childhood, and then at adulthood decreased slightly. In the temporal lobe, $Na_v1.2$ IR neurons peaked at the late fetal stage, and sustained that level during subsequent developmental stages; while $Na_v1.2$ IR neurites increased gradually over all the subjects' developmental stages.

There are a few papers that have reported that $Na_v1.1$ and $Na_v1.2$ could be detected in the rodent and human brains on the mRNA and protein level (Beckh et al., 1989; Black et al., 1994; Felts et al., 1997; Gordon et al., 1987; Jarnot and Corbett, 2006; Westenbroek et al., 1989; Whitaker et al., 2000, 2001b), indicating that they may have common functions across species. For most of previous papers, they have only examined the distribution of $Na_v1.1$ and $Na_v1.2$ on the mRNA level, which are mainly consistent with our sub-regional distribution shown by IHC, and identified the distribution of Nav1.1 and Nav1.2 in the hippocampus and temporal lobe. These findings are common phenomenon in different species. In Jarnot's paper, they report the same cellular distribution of $Na_v1.2$ with us—in both somata and neurites; but the sub-regional distribution are different, they report that $Na_v1.2$ predominately localized in unmyelinated fibers and only localized in a cell body in a small brain region other than the hippocampus in the rat brain (Jarnot and Corbett, 2006). We found $Na_v1.2$ localized in both somata and neurites in each sub-region of the human hippocampus and temporal lobe. These differences in sub-regional distribution may be for the species variation. In Gordon's paper, they compare the expression of Nav1.1 and Nav1.2 in a different brain region, and find that the expression of Nav1.2 is much higher than Nav1.1 in the hippocampus and cerebral cortex, well consistent with our results (Gordon et al., 1987). This conservation of the relative ratio of $Na_v1.1$ and $Na_v1.2$ between different species may represent the common stable function in different species. In the cortex of the temporal lobe, $Na_v1.1$ was obvious in layer IV (the inhibitory layer) and $Na_v1.2$ in layers III and V (the excitatory layers); this difference in distribution may reflect their distinct roles in the human brain. The developmental changes of $Na_v1.1$ and $Na_v1.2$ in the human brain were somewhat different from previous rodent findings (Beckh et al., 1989; Felts et al., 1997; Gazina et al., 2010; Liao et al., 2010), perhaps because of species variation.

There is a report that $Na_v1.7$ has opposing functions in different neuron types, and that these are determined by the existence of another subtype of sodium channel, $Na_v1.8$ (Rush et al., 2006). Similarly, if $Na_v1.1$ or $Na_v1.2$ affect or are affected by other channels, their developmental changes may have their functions altered. $Na_v1.1$ and $Na_v1.2$ neuronal expressions reached their peaks and varied most dramatically during our subjects' first year of life. This being so, $Na_v1.1$ and $Na_v1.2$ may well play a very important role during this period. This could be the reason most sodium channel related epilepsies begin during the first year of life. Dravet syndrome, one of the most important $Na_v1.1$-related epilepsies, is well-known for its intractable treatment. Knowing how critical the first year is, however, we

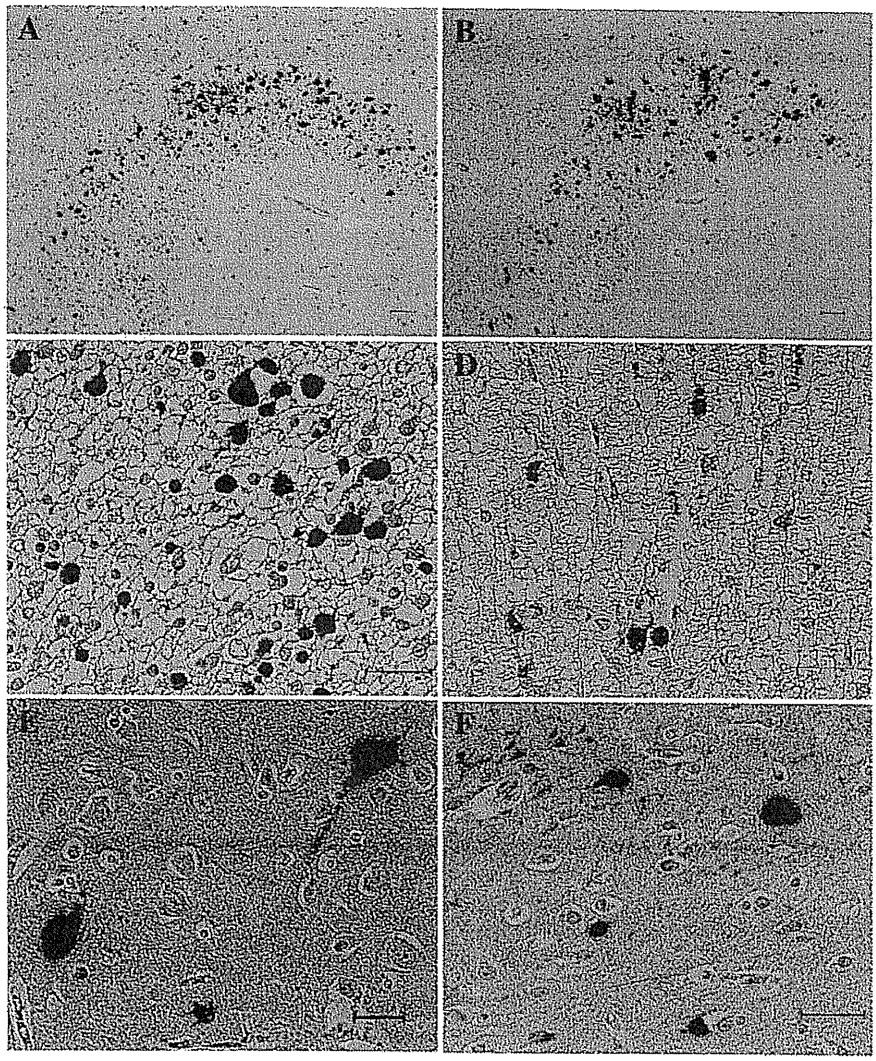

Fig. 3 – The representative pictures of double-staining. A, $Na_v1.2$ mono-staining in the hippocampus from one 22GW case. B, $Na_v1.2$-parvalbumin double-staining using a serial section from the same case with A. The immunoreactivity of A and B are mainly consistent; proving that the double-staining is reliable. C, Local magnification of B. Most $Na_v1.2$ mono-stained (red color) neurons are overlapped with parvalbumin mono-stained (dark-black color) neurons. $Na_v1.2$ immunoreactivity seems more intense in the periphery of the somata, while parvalbumin is in the center. D, $Na_v1.2$-parvalbumin double-staining in the white matter of the temporal lobe from the same case. The double-staining pattern is similar to the hippocampus, although the staining is weak. E, $Na_v1.1$-parvalbumin double-staining in the hippocampus of one 7M infant case. One $Na_v1.1$ mono-stained neuron (red) and two double-stained neurons (purple) are scattered. F, $Na_v1.1$-parvalbumin double-staining in layer IV of the temporal lobe, the same case with E. Several parvalbumin mono-stained neurons (dark blue) and three double-stained neurons (purple) are in the central part, scattered double-stained neurites (arrowhead) in the upper-left corner. Bar: A, B, E, 50 μm; Others, 30 μm.

might do well to begin superactive treatment earlier for infants suffering from Dravet syndrome. We might even use such treatment for infants with *SCN1A* abnormalities before the severe symptoms present, to help them pass through the critical first year of life. This might alleviate the irreversible brain injuries caused by $Na_v1.1$-derived epilepsy. Such a strategy could be explored using any of the several mouse models currently available. If successful, the infants suffering from Dravet syndrome may avoid facing the predetermined doom.

Using double-staining IHC, we studied $Na_v1.1$ and $Na_v1.2$'s colocalization with parvalbumin. Parvalbumin is found in the fast-firing inhibitory interneurons and is considered an excellent chemical marker because of the high quality of its immunoreactivity. Consistent with Ogiwara et al's. (2007) report using a mouse model, our study showed that Nav1.1 and $Na_v1.2$ have high colocalization rates with parvalbumin. Both support the hypothesis derived from mouse models in suggesting that mutations of voltage-gated sodium channels predominantly impair sodium channel activity in interneurons and can cause epilepsy (Martin et al., 2010; Ogiwara et al., 2007; Yu et al., 2006). $Na_v1.1$ and $Na_v1.2$ colocalization rates show different developmental changes; for example, in the

Table 2 – The microscopic analysis results of $Na_v1.2$ immunostaining in the hippocampus and temporal lobe.

Age group	Hippocampus				Temporal cortex (layer)												Temporal white matter	
	Comu ammonis		Dentate gyrus		I		II		III		IV		V		VI			
	Neuron	Neurite	Neuron	Neurite	Neuron	Neurite	Neuron	Neurite	Neuron	Neurite	Neuron	Neurite	Neuron	Neurite	Neuron	Neurite	Neuron[a]	Neurite
13GW–17GW	–	–	–	–	–	–	–	–	–	–	×	×	×	×	×	×	–	–
19GW–22GW	+	+	+	+	±	±	+	±	+	±	×	×	×	×	×	×	+	±
27GW–39GW	++	+	++	+	+1/2	++	++	++	++	++	+	++	++	++	+	+	+	++
P1D–1M	++1/2	+	++	+	++	++	+	++	++	++	+	++	++	++	++	++	+	++
1M–2M	++1/2	++	++	++	++	++	+	++	++	++	+	++	++	++	++	++	+	++
7M–9M	+++	++	+++	+++	++	++	++	++	++	+++	+	++	++	++	++	++	+	++
1Y–5Y	+++	+++	+++	+++	++	++	++	++	++	+++	+	++	++	++	++	++	+	++
46Y–63Y	++	+++	++	+++	++	++	+	++	++	+++	+	++	++	++	++	++	+	++

×, no such recognizable layer.
[a] The scattered neurons in white matter.

Table 3 – The developmental changes of the colocalization rate of $Na_v1.1$ and parvalbumin double-staining in the hippocampus and temporal lobe.

Age group	Hippocampus (CA)	Temporal cortex (layer IV)	Temporal white matter
13GW–19GW	X	X	X
22GW–27GW	49.8% (105/211)	X	65.6% (21/32)
29GW–39GW	49.3% (75/152)	41.9% (13/31)	62.9% (22/35)
P1D–1M	59.0% (79/134)	56.1% (23/41)	48.0% (12/25)
1M–2M	70.7% (70/99)	74.0% (37/50)	39.1% (9/23)
7M–9M	80.3% (61/76)	98.6% (72/73)	X
1Y–5Y	79.5% (62/78)	98.5% (70/71)	X
46Y–63Y	79.3% (65/82)	96.0% (73/76)	X

"X" indicates no colocalization.

hippocampus, the colocalization rate of $Na_v1.1$ and parvalbumin increased from 49.8% at 22GW to 80.4% at 7M, while the colocalization rate of $Na_v1.2$ and parvalbumin was nearly stable during development. These differences may represent variations between different sodium channel subtypes.

After 2M, both $Na_v1.1$ and $Na_v1.2$ showed homogeneous colocalization with parvalbumin in cellular distribution. This is different from Ogiwara et al.'s (2007) report, in which "Nav1.1 is clustered predominantly at the axon initial segments of parvalbumin-positive interneurons". This may be the true variation between species. Both $Na_v1.1$ and $Na_v1.2$ showed relatively obvious colocalization in layer IV of the temporal lobe—where parvalbumin is predominantly expressed (Iai and Takashima, 1999). At the same time, they also showed coincidental developmental changes in cellular distribution patterns, which are related to the characteristic developmental changes of parvalbumin and sodium channels.

Most previous papers suggest that $Na_v1.2$ specifically localizes in axons and terminals (Beckh et al., 1989; Black et al., 1994; Felts et al., 1997; Gordon et al., 1987; Westenbroek et al., 1989; Whitaker et al., 2000, 2001b), although a few did indicate that $Na_v1.2$ expresses in neuronal somata in small regions of rat and cat brains (Gong et al., 1999; Jamot and Corbett, 2006). In this study, we found similar somatic $Na_v1.2$ expression in each subregion of the hippocampus and the temporal lobe. In addition,

Table 4 – The developmental changes of the colocalization rate of $Na_v1.2$ and parvalbumin double-staining in the hippocampus and temporal lobe.

Age group	Hippocampus (CA)	Temporal cortex (layer IV)	Temporal white matter
13GW–19GW	X	X	X
22GW–27GW	81.5% (154/189)	X	75.0% (51/68)
29GW–39GW	81.7% (156/191)	51.4% (36/70)	74.2% (46/62)
P1D–1M	81.3% (139/171)	62.9% (56/89)	47.4% (27/57)
1M–2M	76.1% (153/201)	80.2% (97/121)	41.8% (23/55)
7M–9M	80.4% (189/235)	98.1% (153/156)	X
1Y–5Y	80.1% (185/231)	97.3% (146/150)	X
46Y–63Y	78.2% (179/229)	95.7% (135/141)	X

"X" indicates no colocalization.

we detected scattered $Na_v1.1$ and $Na_v1.2$ IR neurons in the white matter of the temporal lobe. These neurons appeared very early (at 19GW), showed no obvious developmental changes, and were not described in the only previous human brain immunostaining study (Whitaker et al., 2001b). This indicates that sodium channels may have a more complex and extensive distribution pattern than previously thought. The double-staining showed that these neurons were positive for $Na_v1.1$ and $Na_v1.2$, but negative for parvalbumin after 2M, indicating that they may be a sub-population of excitatory neurons having particular functions. In the future, it will be necessary to confirm their exact localizations as well as functions in the human brain.

In conclusion, our study describes the distribution and developmental changes of two sodium channels subtypes—$Na_v1.1$ and $Na_v1.2$—and their colocalization with parvalbumin in the human hippocampus and the temporal lobe. Our results revealed that $Na_v1.1$ and $Na_v1.2$ were heterogeneous in distribution, and showed diverse developmental changes and colocalization patterns with parvalbumin. These may reflect the distinct functions of $Na_v1.1$ and $Na_v1.2$ in the human brain and help us discover the pathomechanisms of age-dependent epilepsies. Furthermore, a detailed study in more human specimens is required and with a novel improvement in the current methods of high-throughput quantitative histological analysis.

4. Experimental procedures

4.1. *Patient samples*

Human post-mortem brain tissues from 28 cases, ranging from 13 weeks of gestation (GW) to 63 years of age (Y), were used. None of the cases had a history of neurological or psychiatric disease. Neutral formalin fixed paraffin embedded brain tissue blocks were cut into 4 μm-thick sections and heated at 45 °C for 10 h for next use. Informed consent was provided in writing by the patients or their family representatives in all cases. The experimental design was reviewed and approved by the Ethics Committee of Fukuoka University.

To guarantee the quality, a neuropathologist reviewed all the autopsy sections, confirmed that the morphology was normal and that they were suitable for immunohistochemistry (IHC). As an additional safeguard, most of the cases had been successfully used in previous IHC research (Kanaumi et al., 2006, 2008).

4.2. *Mono-staining IHC*

The sections were deparaffinized and rehydrated as usual, and then microwaved in 10 mM citrate acid, PH 6.0. for 10 min, and next incubated in turn in 3% skim milk and in 3% H_2O_2 for 10 min at room temperature (RT), rabbit anti-$Na_v1.1$ (1:400; Alomone Labs, Israel) antibody for 2 h RT or rabbit anti-$Na_v1.2$ (1:500; Novus Biologicals, USA) antibody for overnight (O.N.) at 4 °C. Then the sections were incubated with peroxidase-labeled polymer-based universal secondary antibody-goat anti-rabbit and mouse (Nichirei, Japan), 30 min RT, next detected by 3, 3′-diaminobenzidine tetrahydrochloride (DAB) (Sigma, USA). During each change, sections were washed carefully by TBS buffer. Finally the sections were counter-stained with hematoxylin, and dehydrated, cleared and mounted as usual.

4.3. *Double-staining IHC*

We used the sequential method for double-staining. For the first detection, after the same pretreatment as described above, the sections were incubated with rabbit anti-$Na_v1.1$ or rabbit anti-$Na_v1.2$ antibody, then incubated with biotinylated goat anti-rabbit secondary antibody (1:200; Vector, USA) for 45 min RT, and then streptavidin/AP (1:100; Vector, USA) for 45 min RT. They were next detected by New Fuchsin solution (Sigma, USA) (interact with Naphthol AS-BI Phosphate), and then post-fixed in 10% neutral formalin solution for 20 min.

For the second detection, the sections were microwaved again, and then incubated in turn in 3% skim milk, 3% H_2O_2, parvalbumin (1:1000; LifeSpan Biosciences, USA), biotinylated horse anti-mouse polyclonal secondary antibody (1:200; Vector, USA), and streptavidin/HRP (1:100; Dako, USA), as before. Then the sections were detected by DAB-Cobalt solution (Sigma, USA). Finally these were dehydrated, cleared and mounted as usual.

Control experiments (including a block with a corresponding inducing peptide, leaving out the primary antibody and the secondary antibody respectively) were carefully designed and tested to exclude the potential unspecific reaction(s).

4.4. *Microscopic semi-quantitative analysis*

All the sections were viewed carefully under microscope (BX50, Olympus) by two observers. The immunoreactive (IR) neurons were semi-quantitatively evaluated for at least 20HPF (high power field) for each sub-region and graded as negative (−: no specific staining), uncertain (±: undefined staining), mild (+: less than 50% neurons were well stained), moderate (2+: more than 50% neurons were well stained), or marked (3+: more than 50% neurons were markedly stained). The IR neurites were graded semi-quantitatively as negative (−: no specific staining), uncertain (±: undefined staining), mild (+: few neurites were well stained), moderate (2+: some neurites were well stained), or marked (3+: many neurites were markedly stained). The concordance and reproducibility were kept well between different observers. According to the immunoreactivity and the human developmental stages, all cases were divided into eight age groups.

Acknowledgment

We are indebted to all members of the family for their helpful cooperation in this study. We thank Ms. Takako Umemoto and Hideko Takeda for formatting and typing the manuscript and Ms. Minako Yonetani and Akiyo Hamachi for the technical assistance. This study was supported in part by Grants-in-Aid for Scientific Research (S) 16109006, (A) 18209035 and 21249062, Exploratory Research 1659272, and "High-Tech Research Center" Project for Private Universities-matching fund subsidy from the Ministry of Education, Culture, Sports, Science and Technology, 2006–2010—"The Research Center for the Molecular Pathomechanisms of Epilepsy, Fukuoka University", research grants (19A-6) and (21B-5) for Nervous and Mental Disorders

from the Ministry of Health, Labor and Welfare and the Central Research Institute of Fukuoka University.

Appendix A Supplementary data

Supplementary data to this article can be found online at doi:10.1016/j.brainres.2011.02.083.

REFERENCES

Beckh, S., Noda, M., Lubbert, H., Numa, S., 1989. Differential regulation of three sodium channel messenger RNAs in the rat central nervous system during development. EMBO J. 8, 3611–3616.

Black, J.A., Yokoyama, S., Higashida, H., Ransom, B.R., Waxman, S. G., 1994. Sodium channel mRNAs I, II and III in the CNS: cell-specific expression. Brain Res. Mol. Brain Res. 22, 275–289.

Clare, J.J., Tate, S.N., Nobbs, M., Romanos, M.A., 2000. Voltage-gated sodium channels as therapeutic targets. Drug Discov. Today 5, 506–520.

Felts, P.A., Yokoyama, S., Dib-Hajj, S., Black, J.A., Waxman, S.G., 1997. Sodium channel alpha-subunit mRNAs I, II, III, NaG, Na6 and hNE (PN1): different expression patterns in developing rat nervous system. Brain Res. Mol. Brain Res. 45, 71–82.

Fukuma, G., Oguni, H., Shirasaka, Y., Watanabe, K., Miyajima, T., Yasumoto, S., Ohfu, M., Inoue, T., Watanachai, A., Kira, R., Matsuo, M., Muranaka, H., Sofue, F., Zhang, B., Kaneko, S., Mitsudome, A., Hirose, S., 2004. Mutations of neuronal voltage-gated Na+ channel alpha 1 subunit gene SCN1A in core severe myoclonic epilepsy in infancy (SMEI) and in borderline SMEI (SMEB). Epilepsia 45, 140–148.

Gazina, E.V., Richards, K.L., Mokhtar, M.B., Thomas, E.A., Reid, C.A., Petrou, S., 2010. Differential expression of exon 5 splice variants of sodium channel alpha subunit mRNAs in the developing mouse brain. Neuroscience 166, 195–200.

Gong, B., Rhodes, K.J., Bekele-Arcuri, Z., Trimmer, J.S., 1999. Type I and type II Na(+) channel alpha-subunit polypeptides exhibit distinct spatial and temporal patterning, and association with auxiliary subunits in rat brain. J. Comp. Neurol. 412, 342–352.

Gordon, D., Merrick, D., Auld, V., Dunn, R., Goldin, A.L., Davidson, N., Catterall, W.A., 1987. Tissue-specific expression of the RI and RII sodium channel subtypes. Proc. Natl. Acad. Sci. U. S. A. 84, 8682–8686.

Iai, M., Takashima, S., 1999. Thalamocortical development of parvalbumin neurons in normal and periventricular leukomalacia brains. Neuropediatrics 30, 14–18.

Jarnot, M., Corbett, A.M., 2006. Immunolocalization of NaV1.2 channel subtypes in rat and cat brain and spinal cord with high affinity antibodies. Brain Res. 1107, 1–12.

Kanaumi, T., Takashima, S., Iwasaki, H., Mitsudome, A., Hirose, S., 2006. Developmental changes in the expression of GABAA receptor alpha 1 and gamma 2 subunits in human temporal lobe, hippocampus and basal ganglia: an implication for consideration on age-related epilepsy. Epilepsy Res. 71, 47–53.

Kanaumi, T., Takashima, S., Iwasaki, H., Itoh, M., Mitsudome, A., Hirose, S., 2008. Developmental changes in KCNQ2 and KCNQ3 expression in human brain: possible contribution to the age-dependent etiology of benign familial neonatal convulsions. Brain Dev. 30, 362–369.

Kaneko, Y., Watanabe, S., 2007. Expression of Nav1.1 in rat retinal AII amacrine cells. Neurosci. Lett. 424, 83–88.

Kumakura, A., Ito, M., Hata, D., Oh, N., Kurahashi, H., Wang, J.W., Hirose, S., 2009. Novel de novo splice-site mutation of SCN1A in a patient with partial epilepsy with febrile seizures plus. Brain Dev. 31, 179–182.

Liao, Y., Deprez, L., Maljevic, S., Pitsch, J., Claes, L., Hristova, D., Jordanova, A., Ala-Mello, S., Bellan-Koch, A., Blazevic, D., Schubert, S., Thomas, E.A., Petrou, S., Becker, A.J., De Jonghe, P., Lerche, H., 2010. Molecular correlates of age-dependent seizures in an inherited neonatal–infantile epilepsy Brain 133, 1403–1414.

Lu, C.M., Han, J., Rado, T.A., Brown, G.B., 1992. Differential expression of two sodium channel subtypes in human brain. FEBS Lett. 303, 53–58.

Martin, M.S., Dutt, K., Papale, L.A., Dube, C.M., Dutton, S.B., de Haan, G., Shankar, A., Tufik, S., Meisler, M.H., Baram, T.Z., Goldin, A.L., Escayg, A., 2010. Altered function of the SCN1A voltage-gated sodium channel leads to {gamma}-aminobutyric acid-ergic (GABAergic) interneuron abnormalities. J. Biol. Chem. 285, 9823–9834.

Oakley, J.C., Kalume, F., Yu, F.H., Scheuer, T., Catterall, W.A., 2009. Temperature- and age-dependent seizures in a mouse model of severe myoclonic epilepsy in infancy. Proc. Natl. Acad. Sci. U. S. A. 106, 3994–3999.

Ogiwara, I., Miyamoto, H., Morita, N., Atapour, N., Mazaki, E., Inoue, I., Takeuchi, T., Itohara, S., Yanagawa, Y., Obata, K., Furuichi, T., Hensch, T.K., Yamakawa, K., 2007. Na(v)1.1 localizes to axons of parvalbumin-positive inhibitory interneurons: a circuit basis for epileptic seizures in mice carrying an Scn1a gene mutation. J. Neurosci. 27, 5903–5914.

Rush, A.M., Dib-Hajj, S.D., Liu, S., Cummins, T.R., Black, J.A., Waxman, S.G., 2006. A single sodium channel mutation produces hyper- or hypoexcitability in different types of neurons. Proc. Natl. Acad. Sci. U. S. A. 103, 8245–8250.

Shi, X., Yasumoto, S., Nakagawa, E., Fukasawa, T., Uchiya, S., Hirose, S., 2009. Missense mutation of the sodium channel gene SCN2A causes Dravet syndrome. Brain Dev. 31, 758–762.

Sugawara, T., Mazaki-Miyazaki, E., Ito, M., Nagafuji, H., Fukuma, G., Mitsudome, A., Wada, K., Kaneko, S., Hirose, S., Yamakawa, K., 2001. Nav1.1 mutations cause febrile seizures associated with afebrile partial seizures Neurology 57, 703–705.

Tang, B., Dutt, K., Papale, L., Rusconi, R., Shankar, A., Hunter, J., Tufik, S., Yu, F.H., Catterall, W.A., Mantegazza, M., Goldin, A.L., Escayg, A., 2009. A BAC transgenic mouse model reveals neuron subtype-specific effects of a Generalized Epilepsy with Febrile Seizures Plus (GEFS+) mutation. Neurobiol. Dis. 35, 91–102.

Vacher, H., Mohapatra, D.P., Trimmer, J.S., 2008. Localization and targeting of voltage-dependent ion channels in mammalian central neurons. Physiol. Rev. 88, 1407–1447.

Van Wart, A., Trimmer, J.S., Matthews, G., 2007. Polarized distribution of ion channels within microdomains of the axon initial segment. J. Comp. Neurol. 500, 339–352.

Wang, J.W., Kurahashi, H., Ishii, A., Kojima, T., Ohfu, M., Inoue, T., Ogawa, A., Yasumoto, S., Oguni, H., Kure, S., Fujii, T., Ito, M., Okuno, T., Shirasaka, Y., Natsume, J., Hasegawa, A., Konagaya, A., Kaneko, S., Hirose, S., 2008. Microchromosomal deletions involving SCN1A and adjacent genes in severe myoclonic epilepsy in infancy. Epilepsia 49, 1528–1534.

Westenbroek, R.E., Merrick, D.K., Catterall, W.A., 1989. Differential subcellular localization of the RI and RII Na+ channel subtypes in central neurons. Neuron 3, 695–704.

Whitaker, W.R., Clare, J.J., Powell, A.J., Chen, Y.H., Faull, R.L., Emson, P.C., 2000. Distribution of voltage-gated sodium channel alpha-subunit and beta-subunit mRNAs in human hippocampal formation, cortex, and cerebellum. J. Comp. Neurol. 422, 123–139.

Whitaker, W.R., Faull, R.L., Dragunow, M., Mee, E.W., Emson, P.C., Clare, J.J., 2001a. Changes in the mRNAs encoding voltage-gated sodium channel types II and III in